The inhibiting effect of some Quinoxaline derivative towards mild steel corrosion in acid media: Chemical, Electrochemical and Theoretical studies

J. Saranya[1], P. Sounthari[1], A. Kiruthuka[1], K. Parameswari[1], S. Chitra[1*]

[1]*Department of Chemistry, PSGR Krishnammal College for Women, Coimbatore, India*

Abstract

Corrosion inhibition of mild steel in 1 M H_2SO_4 was investigated in the absence and presence of different concentrations of quinoxaline derivatives namely (3E)-3-(phenylimino)-3,4-dihydroquinoxalin-2(1H)-one (PDQO), (3E)-3-[(2-methylphenyl)imino]-3,4-dihydroquinoxalin-2(1H)-one (MPDQO) and (3E)-3-[(2-methoxy-phenyl)imino]-3,4-dihydroquinoxalin-2(1H)-one (MOPDQO). Weight loss, potentiodynamic polarization and electrochemical impedance spectroscopy (EIS) measurements were employed. Impedance measurements showed that the charge transfer resistance increased and double layer capacitance decreased with increase in the inhibitor concentration. Potentiodynamic polarization study showed that the inhibitors acted as mixed-type inhibitors. The adsorption of these compounds on the mild steel surface obeys a Langmuir adsorption isotherm. Results obtained reveal that compound MOPDQO is the best inhibitor and the inhibition efficiency follows the sequence: MOPDQO > MPDQO > PDQO. Electronic properties such as highest occupied molecular orbital (E_{HOMO}) and lowest unoccupied molecular orbital (E_{LUMO}), the energy difference (ΔE) between E_{HOMO} and E_{LUMO}, dipole moment (μ), electronegativity (χ), electron affinity (A), hardness (η), softness (σ), ionization potential (I), the fraction of electrons transferred (ΔN), total energy (TE) were calculated and discussed. The results showed that the corrosion inhibition efficiency increased with an increase in the E_{HOMO} values but decrease in the E_{LUMO} values. Mulliken atomic charges, Fukui functions and softness indices were discussed in order to characterize the inhibition property of the inhibitors.

Keywords: Corrosion rate, Impedance, Isotherm, Quinoxaline, Weight loss.

1. Introduction

Mild steel finds a variety of applications industrially, for mechanical and structural purposes, like bridge work, building, boiler parts, steam engine parts and automobiles. It finds various uses in most of the chemical industries due to its low cost and easy availability for fabrication of various reaction vessels, tanks, pipes, etc. Since it suffers from severe corrosion in aggressive environment, it has to be protected. Acids like H_2SO_4 and HCl have been used for drilling operations, pickling baths and in descaling processes.

Corrosion of mild steel and its alloys in different acid media have been extensively studied [1-6]. It has been reported that addition of heteroatoms, retards the corrosion of mild steel in acidic environments [7-8]. They act by adsorption on the metal surface which takes place through heteroatoms such as N, O, P and S atoms, triple bonds or aromatic rings which tend to form stronger coordination bonds. Among the various heterocyclic compounds studied as inhibitors, quinoxalines have been considered as environmentally acceptable chemicals. The continuation of our work on development of organic compounds as acid inhibitors is oriented to a new series of quinoxaline compounds. Many of the substituted quinoxaline compounds have been recently studied in considerable detail as effective corrosion inhibitors for steel and copper in acidic media [9-14]. The good inhibitory effect of quinoxaline derivatives [15-17] has incited us to test 1,4-dihydroquinoxaline-2,3-dione derivatives as corrosion inhibitors for mild steel in 1M H_2SO_4 in the range 303 - 333 K.

In order to support the experimental data, theoretical calculations were conducted in order to provide molecular-level understanding of the observed experimental behavior. Among quantum chemical methods for evaluation of corrosion inhibitors, density functional theory (DFT) has shown significant promise and appears to be adequate for pointing out the changes in electronic structure responsible for inhibitory action [18]. In order to evaluate compounds as corrosion inhibitors and design novel one, the relationship between the structural properties of the molecules and their inhibition effects is being explored. Various organic compounds have been investigated for their inhibiting behavior and their molecular structures have also been studied by quantum chemical methods in order to elucidate the origins of their inhibition effect [19-21].

The first objective of this work is to report the effect of quinoxaline derivatives as corrosion inhibitors in 1M H_2SO_4 medium using weight loss, potentiodynamic polarization and AC-impedance spectroscopy methods. The second objective is to investigate the dependence of inhibition efficiency of these compounds on theoretical chemical parameters such as the energies of the highest occupied molecular orbital (E_{HOMO}) and the lowest unoccupied molecular orbital (E_{LUMO}), the energy difference (ΔE) between E_{HOMO} and E_{LUMO}, dipole moment (μ), electronegativity (χ), electron affinity (A), global hardness (η), softness (σ), ionization potential (I), the fraction of electrons transferred (ΔN), total energy (TE), Mulliken atomic charges, Fukui functions and softness indices to characterize the inhibition property of the inhibitors.

2.   Materials and Methods
Cold rolled mild steel specimen of size 1cm x 3cm x 0.08cm having composition 0.084% C, 0.369% Mn, 0.129% Si, 0.025% P, 0.027% S, 0.022% Cr, 0.011% Mo, 0.013% Ni and the reminder iron were used for weight loss measurements. For electrochemical methods, a mild steel rod of same composition with an exposed area of 0.785 cm^2 was used. The specimens were polished with 1/0, 2/0, 3/0 and 4/0 grades of emery sheets and degreased with trichloroethylene and dried using a drier. The plates were kept in a desiccator to avoid the absorption of moisture.

*2.1. Synthesis of the inhibitor*
Step 1: Synthesis of 1,4-dihydroquinoxaline-2,3-dione (1)
        A mixture of oxalic acid (6.5 g) and o-phenylenediamine   (5.5 g) were dissolved in 4N HCl. The solution was allowed to boil for 15 minutes. A crystalline solid appeared which was cooled, washed with water and dried. The compound was dissolved in alkali and acidified with HCl. Pure 1,4-dihydroquinoxaline-2,3-dione was obtained as white needles. Yield: 3g. Melting point: >350^{0}C.
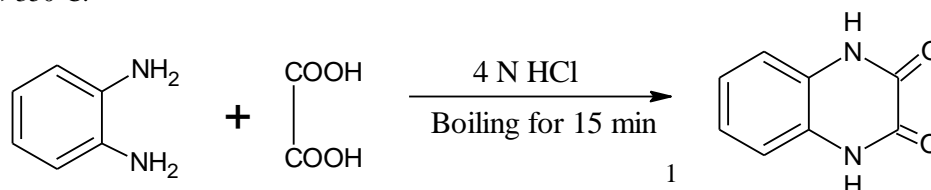
Step 2: Synthesis of 1,4-dihydroquinoxaline-2,3-dione derivative (2$_{a-c}$)
        A mixture of the 1,4-dihydroquinoxaline-2,3-dione (1 mole), amine (NH_2-NH_2/urea/thiourea) (1 mole) and ethanol (50 ml) were heated under reflux for 2 hour, then cooled to room temperature. The precipitate was filtered, washed with water and recrystallized from 2-butanol.
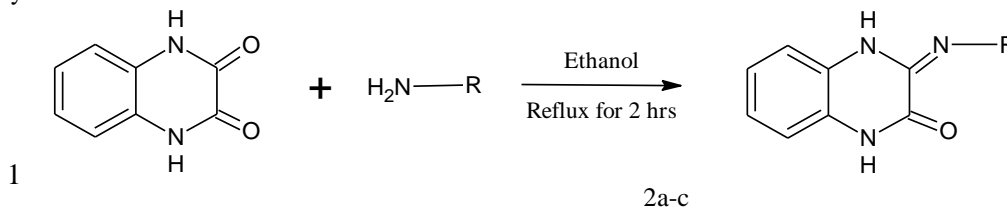
R= -C_6H_5,-$C_6H_5CH_3$, -$C_6H_5OCH_3$
(3E)-3-(phenylimino)-3,4-dihydroquinoxalin-2(1H)-one (PDQO) 2a: Yield: 70%, Melting Point = 318 - 320ºC, white solid, IR Spectrum   (γ/cm^{-1}) : 1673.32 (C=N); 1747.80 (C=O); 1230.01 (C-N)
(3E)-3-[(2-methylphenyl)imino]-3,4-dihydroquinoxalin-2(1H)-one (MPDQO) 2b: Yield: 74%, Melting Point = 278 - 280ºC, brown solid, IR Spectrum (γ/cm^{-1}) : 1672.36 (C=N); 1746.62 (C=O); 1219.06 (C-N)
(3E)-3-[(2-methoxyphenyl)imino]-3,4-dihydroquinoxalin-2(1H)-one (MPDQO) 2c: Yield: 78%, Melting Point = 312 - 314ºC, pale brown solid, IR Spectrum (γ/cm^{-1}) : 1674.28 (C=N); 1739.87 (C=O); 1220.03 (C-N)

2.2 Non-Electrochemical Techniques
2.2.1. Weight loss method
        The initial weight of the polished mild steel plates of size 1cm x 3cm x 0.08cm was taken. The solutions were taken in a 100 ml beaker and the specimens were suspended in triplicates into the solution using glass hooks. Care was taken to ensure the complete immersion of the specimen. After a period of 3 hours the specimens were removed, washed with distilled water, dried and weighed.
From the initial and final masses of the plates (i.e., before and after immersion in the solution) the loss in weight was calculated. The experiment was repeated for various inhibitor concentrations in 1M H_2SO_4. A blank was carried out without inhibitor.
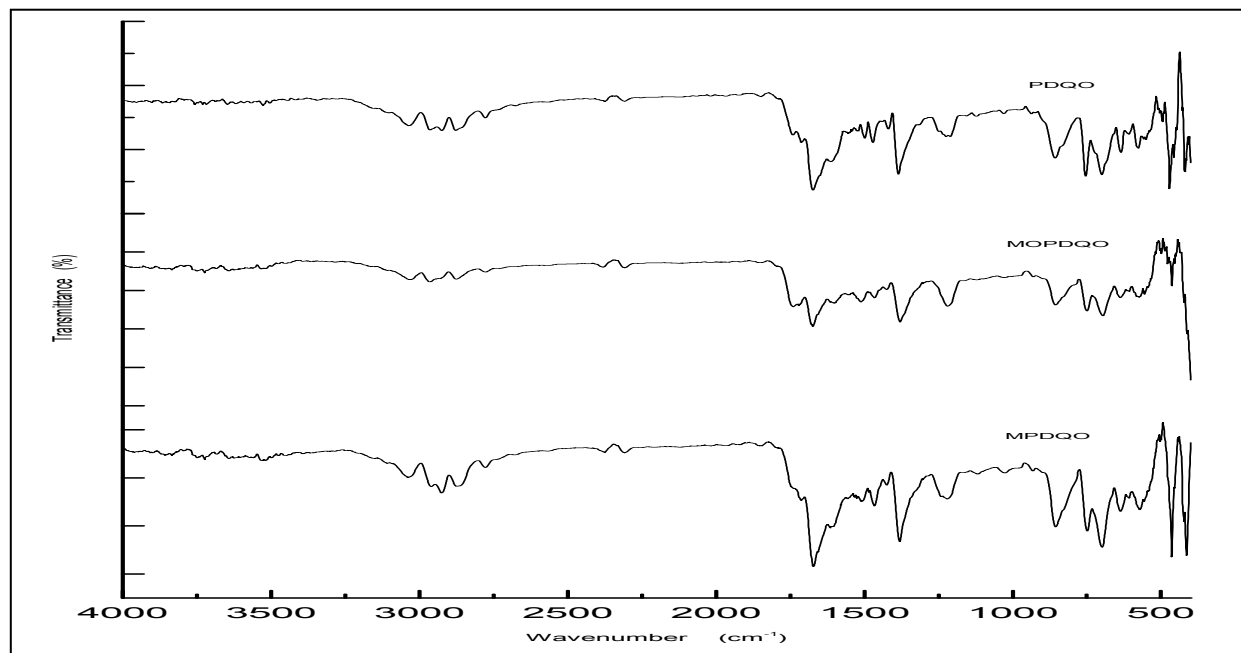
Figure 1: FT-IR Spectra of the synthesized compounds

The inhibition efficiency, corrosion rate and surface coverage were calculated from the weight loss results using the formulas:

$$\text{Efficiency of inhibitor} = \frac{(\text{Weight loss without inhibitor} - \text{Weight loss with inhibitor})}{\text{Weight loss without inhibitor}} \times 100$$

$$\text{Corrosion Rate} = \frac{534 \times \text{Weight loss (g)}}{\text{Density} \times \text{Area (cm)} \times \text{Time (hr)}}$$

$$\text{Surface Coverage } \theta = \frac{((\text{Weight loss without inhibitor}) - (\text{Weight loss with inhibitor}))}{\text{Weight loss without inhibitor}}$$

To study the effect of temperature, the above procedure was carried out at different temperature range i.e., (313-333K) using thermostat with the inhibitor concentration of 10mM.

Activation energy (E_a), Free energy of adsorption (ΔG^0), Enthalpy and Entropy (ΔH^0 & ΔS^0) were calculated using the formula,

$$(i) \quad \log CR = \frac{-E_a}{2.303\,RT} + \log A$$

$$(ii) \quad K = \frac{1}{55.5} \exp\left[-\frac{\Delta G^{\circ}_{ads}}{RT}\right]$$

where $K = \dfrac{\theta}{c(1-\theta)}$ [from Langmuir equation], θ - Surface coverage of the inhibitor, C- concentration of inhibitor in mM/100ml

$$(iii) \quad CR = \frac{RT}{Nh} \exp\frac{\Delta S^{\circ}}{R} \exp\frac{-\Delta H^{\circ}}{RT}$$

h – Planck's constant, N - Avogadro number, T - Absolute temperature, R - Universal gas constant.

2.3 Electrochemical Techniques

Electrochemical impedance spectroscopy (EIS) and Potentiodynamic polarization were carried out with IVIUM Compactstat Potentiostat/Galvanostat. EIS measurements were carried out at a frequency range of 10 KHz to 0.01Hz with a superimposed sine wave of amplitude 10mV. From the plot of Z^1 Vs Z^{11} the charge transfer resistance (R_{ct}) and double layer capacitance (C_{dl}) were calculated. The inhibition efficiency was calculated using the formula

$$\text{Inhibition Efficiency (\%)} = \frac{R^{*}_{ct} - R_{ct}}{R^{*}_{ct}} \times 100$$

where R_{ct} and R_{ct}^{*} are the charge transfer resistance obtained in the absence and presence of the inhibitors.

The potentiodynamic polarization curves were made after EIS for a potential range of -100mV to +100mV (versus OCP) with a scan rate of 1 mV/s .The data were collected and analyzed by IVIUM Soft software. The inhibition efficiency was calculated from the I_{corr} using the formula

$$\text{Inhibition Efficiency } (\%) = \frac{I_{corr} - I_{corr(inh)}}{I_{corr}} X100$$

where I_{corr} and $I_{corr(inh)}$ signifies the corrosion current density in the absence and presence of inhibitors.

2.4 Surface Morphology

Surface examinations of mild steel specimens were carried out to understand the surface morphology of mild steel in 1M H_2SO_4 in the presence and absence of the inhibitors using JEOL Scanning Electron Microscopy (Karunya University, Coimbatore).

2.5 Quantum Chemical Studies

DFT method is very much useful for the Quantum mechanical calculations of energies, geometries and vibrational wave numbers of organic chemical system. The gradient corrected density functional theory (DFT) with the three parameter hybrid functional Becke3 (B3) for the exchange part and the Lee–Yang–Parr (LYP)correlation functional, calculations have been carried out in the present investigation, using 6-311G(d,p) basis sets with Gaussian-03 program, invoking gradient geometry optimization. All the parameters were allowed to relax and all the calculations converged to an optimised geometry which corresponds to true energy minima.

3. Results and discussion

3.1 Non-Electrochemical Measurements

3.1.1 Weight loss measurements

The weight loss measurements are conducted in 1M H_2SO_4 at 303 K for 3hr of immersion time. The values of corrosion rate (CR), surface coverage (θ) and inhibition efficiency (%) containing PDQO, MPDQO and MOPDQO at different concentrations are represented in Table 1.

Table 1: Inhibition efficiencies of various concentrations of the inhibitors for corrosion of mild steel in 1M H_2SO_4 obtained by weight loss measurement at 30 ± 1^0C

Name of the Inhibitor	Con (mM)	Weight loss (g)	Inhibition Efficiency (%)	Surface Coverage (θ)	Corrosion Rate (g cm^{-2}hr^{-1})
BLANK	-	0.2212	-	-	21.92
PDQO	0.5	0.0601	72.83	0.8395	5.96
	1	0.0543	75.45	0.8697	5.38
	2.5	0.0446	79.84	0.9203	4.42
	5	0.0416	81.19	0.9359	4.12
	7.5	0.0353	84.04	0.9687	3.49
	10	0.0293	86.75	1	2.90
MPDQO	0.5	0.0493	77.71	0.8300	4.89
	1	0.0401	81.87	0.8745	3.97
	2.5	0.0326	85.26	0.9107	3.23
	5	0.0241	89.1	0.9517	2.39
	7.5	0.0191	91.37	0.9759	1.89
	10	0.0141	93.63	1	1.39
MOPDQO	0.5	0.0247	88.83	0.9001	2.45
	1	0.0201	90.91	0.9212	1.99
	2.5	0.0173	92.18	0.9340	1.72
	5	0.0084	95.75	0.9748	0.83
	7.5	0.0041	98.15	0.9945	0.41
	10	0.0029	98.69	1	0.29

It is shown that MOPDQO acts as effective corrosion inhibitor. The corrosion suppressing ability of the quinoxaline molecules are probably due to the interaction between π electrons of the two aromatic rings of the quinoxaline, the free pairs of electrons of N and O atoms with the positively charged metal surface and the presence of electron density groups. The order of inhibition efficiency follows:
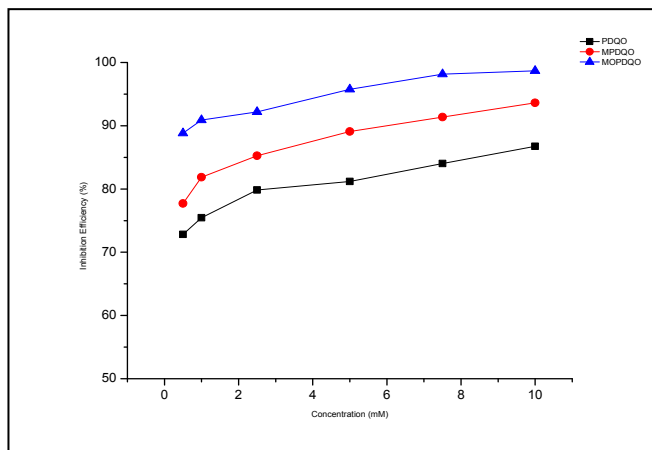
MOPDQO > MPDQO > PDQO

Figure 2: Plot of inhibition efficiency (%) Vs concentration (mM) for the inhibition of corrosion of mild steel in 1M H_2SO_4

3.1.2 Kinetic and Thermodynamic parameters

The effect of temperature on the corrosion of mild steel/acid in the presence and absence of inhibitors at a concentration of 10mM was investigated by weight loss method in the temperature range 303K to 333 K for an immersion period of 1 hour. The results are depicted in Table 2 which implies that inhibition efficiency decreases with increase in temperature.

Table 2: Inhibition efficiencies of 10mM concentrations of the inhibitors for corrosion of mild steel in 1M H_2SO_4 obtained by weight loss measurement at higher temperature

Name of the Inhibitor	Temperature (K)	Weight loss (g)	Inhibition Efficiency (%)	Corrosion rate (g cm^{-2}hr^{-1})
BLANK	303	0.0619	-	18.40
	313	0.1152	-	34.25
	323	0.2247	-	66.81
	333	0.4762	-	141.58
PDQO	303	0.0486	21.49	14.45
	313	0.0962	16.49	28.60
	323	0.1949	13.26	57.95
	333	0.4197	11.86	124.78
MPDQO	303	0.0457	26.17	13.59
	313	0.0912	20.83	27.12
	323	0.1986	11.62	59.05
	333	0.3957	16.90	117.65
MOPDQO	303	0.0473	30.13	14.06
	313	0.0946	26.95	28.13
	323	0.2013	20.31	59.85
	333	0.4261	15.14	126.69
	333	0.4329	13.78	128.71

Temperature increases the rate of all electrochemical processes and influences adsorption equilibrium and kinetics as well. Adsorption and desorption of inhibitor molecules continuously occur at the metal surface and an equilibrium exists between two processes at a particular temperature. With increase in temperature the equilibrium between adsorption and desorption processes is shifted to a higher desorption rate than adsorption until equilibrium is again established at a different value of equilibrium constant. This explains the lower inhibition efficiency at higher value.

In acidic solution the corrosion rate is related to temperature by the Arrhenius equation

$$\log (CR) = \frac{-E_a}{2.303\,RT} X \log A \qquad (1)$$

where E_a is the apparent activation energy and A - frequency factor, R – Gas constant, T – Temperature.
Figure 3 shows the plot of log CR Vs 1/T. Linear plots were obtained for all the inhibitors. The values of E_a were computed from the slope of the straight lines and are listed in Table 4. A plot of ΔG Vs $\frac{1}{T}$ gives straight line with slope $\frac{-\Delta H^{\circ}}{2.303\,R}$ and intercept $\ln \frac{R}{Nh} + \frac{\Delta S^{\circ}}{R}$ from which the values of ΔH^0 and ΔS^0 were calculated and listed in Table 3.

Table 3: Kinetics/Thermodynamic Parameters of mild steel corrosion in 1M H_2SO_4 at different temperatures

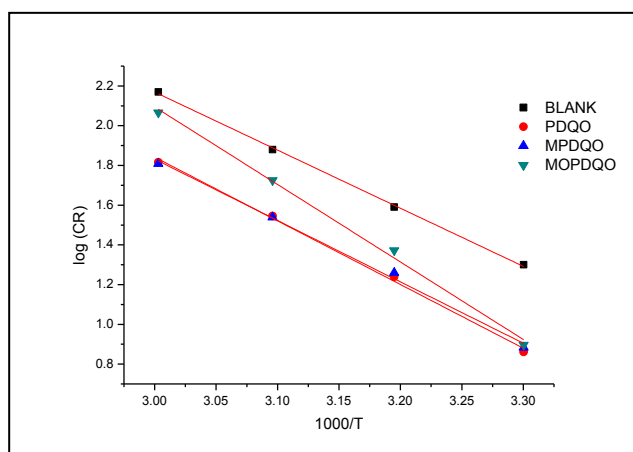| Name of the inhibitor	E_a kJ mol^{-1}	-ΔG kJ mol^{-1}				-ΔH kJ mol^{-1}	-ΔS kJ mol^{-1}
		303	313	323	333		
BLANK	56.86	-	-	-	-	-	-
PDQO	60.11	18.46	18.22	18.11	18.32	30.95	1.65
MPDQO	60.83	19.60	19.84	19.49	19.10	1.53	1.57
MOPDQO	61.60	19.11	18.97	17.71	19.46	109.60	1.91

Figure 3: Arrhenius plot for the inhibition of corrosion of mild steel in 1M H_2SO_4

It is observed that the apparent activation energy is higher in the presence of inhibitor than in its absence. This type of inhibitor retards corrosion at ordinary temperatures but inhibition is diminished at elevated temperature. The negative sign of ΔH^0 reflects the exothermic nature of the corrosion process. The values of E_a and ΔH^0 enhance with an increase in the concentration of the inhibitor suggesting that the energy barrier of corrosion reaction increases as the concentration of inhibitor is increased. This means that the corrosion reaction will further be pushed to surface sites that are characterized by progressively higher values of E_a as the concentration of the inhibitor becomes greater [22]. The entropy of activation, ΔS^0, in the absence and presence of

inhibitor is negative. This implies that, the activated complex in the rate determining step represents association rather than dissociation step, meaning that a decrease in disordering takes place on going from reactants to the activated complex [23,24]. However, this value decreases gradually with increasing inhibitor concentrations.

In the present study, the ΔG^0_{ads} values (Table 4) obtained ranges from -17 to -19 KJ/mol, which are lower than -20 KJ/mol. This indicates that the adsorption is typical physisorption [25]. Thus assumption is supported by the data process reported in Table 3 which shows that inhibition efficiency decreases with increase in temperature (physisorption) [26].

Table 4: Thermodynamic parameters of adsorption of 1,4-dihydroquinoxaline-2,3-dione derivatives on the mild steel surface at room temperature

Name of the Inhibitor	Langmuir Isotherm			Temkin Isotherm		
	R^2	K mol lt^{-1}	$-\Delta G$ kJ mol^{-1}	R^2	K mol lt^{-1}	$-\Delta G$ kJ mol^{-1}
PDQO	0.9988	226.18	23.78	0.9675	755.57	26.82
MPDQO	0.9993	208.00	23.57	0.9905	812.78	27.00
MOPDQO	0.9997	125.94	22.30	0.9474	906.47	27.28

Name of the Inhibitor	Flory-Huggins's Isotherm				El-Awady Isotherm			
	R^2	K mol lt^{-1}	$-\Delta G$ kJ mol^{-1}	1/n	R^2	K mol lt^{-1}	$-\Delta G$ kJ mol^{-1}	1/y
PDQO	0.897	2339.22	29.67	0.25	0.936	492.66	11.19	3.58
MPDQO	0.927	1567.49	28.66	0.44	0.943	644.93	11.48	2.24
MOPDQO	0.860	1116.93	27.80	0.85	0.822	996.41	11.96	1.37

3.1.3 Adsorption Isotherm

Establishment of isotherms that describe the adsorptive behaviour of a corrosion inhibitor is an important part of its study as they can provide important clues to the nature of metal inhibitor concentration. In order to obtain the isotherm, linear relation between θ values and the inhibitor concentration 'C' was found. Attempts were made to fit the θ values to various isotherms including Langmuir, Temkin, Flory-Huggin's and El-Awady. The best fit was obtained with the Langmuir isotherm.

Langmuir adsorption isotherm was found to be the best description of the adsorption behaviour of the studied inhibitors. This adsorption isotherm is described by the following equation

$$\frac{C}{\theta} = \frac{1}{k_{ads}} + C \qquad (3)$$

where k_{ads} is the equilibrium constant of the adsorption process and 'C' is the inhibitor concentration and θ is the fraction of the surface covered. Figure 4 shows the dependence of C/θ as a function of concentration C for the inhibitors.

The inhibitors also obey Temkin adsorption isotherm which is represented in Figure 5, equation (4). The values of adsorption parameters deduced from the plots are tabulated on Table-4.

$$Exp^{-2a\theta} = KC \qquad (4)$$

The relationship between the equilibrium constant, K, of adsorption and the free energy of adsorption, ΔG_{ads}, is given by the following expression

$$\Delta G_{ads} = -2.303RT \log (55.5 K) \qquad (5)$$

The values of free energy of adsorption calculated from equation (5) using K values obtained from the Langmuir adsorption and Temkin adsorption isotherm are presented in Table-2. The values are negative and less than -30 kJmol^{-1}. This implies that the adsorption of the inhibitor on mild steel surface is spontaneous and confirms physical adsorption mechanism [25].
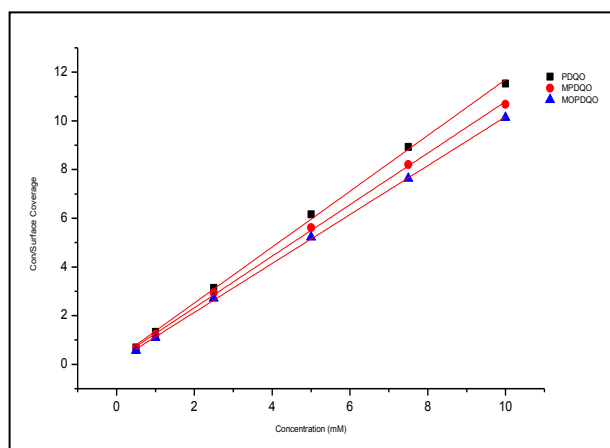
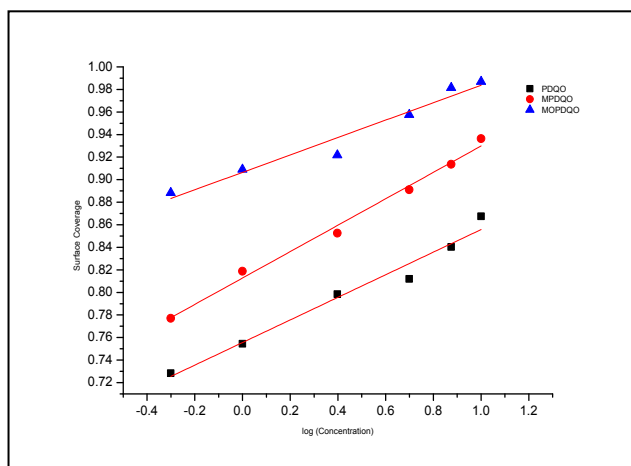**Figure 4**: Langmuir plot for the inhibition of corrosion of mild steel in 1M H_2SO_4

Figure 5: Temkin plot for the inhibition of corrosion of mild steel in 1M H_2SO_4

The inhibitors also obey Temkin adsorption isotherm which is represented in Figure 5, equation (4). The values of adsorption parameters deduced from the plots are tabulated on Table-4.

$$Exp^{-2a\theta} = KC \tag{4}$$

The relationship between the equilibrium constant, K, of adsorption and the free energy of adsorption, ΔG_{ads}, is given by the following expression

$$\Delta G_{ads} = -2.303RT \log (55.5\ K) \tag{5}$$

The values of free energy of adsorption calculated from equation (5) using K values obtained from the Langmuir adsorption and Temkin adsorption isotherm are presented in Table-2. The values are negative and less than -30 kJmol^{-1}. This implies that the adsorption of the inhibitor on mild steel surface is spontaneous and confirms physical adsorption mechanism [25].

The Flory-Huggins adsorption isotherm can be given by the following equation

$$\log \frac{\theta}{c} = \log K + \log (1-\theta) \tag{6}$$

The plots of $\log \dfrac{\theta}{1-\theta}$ against log C gave a linear relationship (Figure 6) showing that Flory-Huggins isotherm was obeyed. The values of the size parameter (y) are positive (Table 5) which indicates that the inhibitor molecules are adsorbed on the mild steel surface by displacing more than one water molecule [26]. By testing other adsorption isotherms, it is found that the experimental data fits the El- Awady adsorption isotherm for the room temperature range studied. The characteristic of the isotherm is given by

$$\log\left(\frac{\theta}{1-\theta}\right) = \log K + y \log C_{inh} \qquad (7)$$

where C_{inh} is molar concentration of inhibitor in the bulk solution, θ is the degree of surface coverage, K is the equilibrium constant of adsorption process ; $K_{ads} = K^{1/y}$ and y represent the number of inhibitor molecules occupying a given active site. Value of 1/y less than unity implies the formation of multilayer of the inhibitor on the metal surface, while the value of 1/y greater than unity means that a given inhibitor occupy more than one active site. [27-29] Curve fitting of the data to the thermodynamic/kinetic model (El-Awady et. al.) is shown in Figure 7.
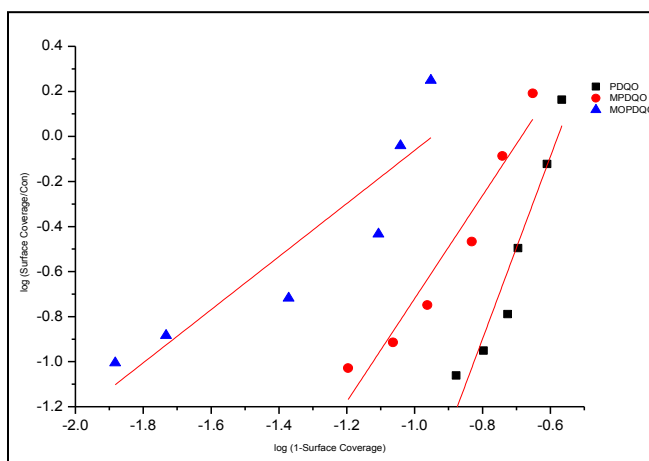

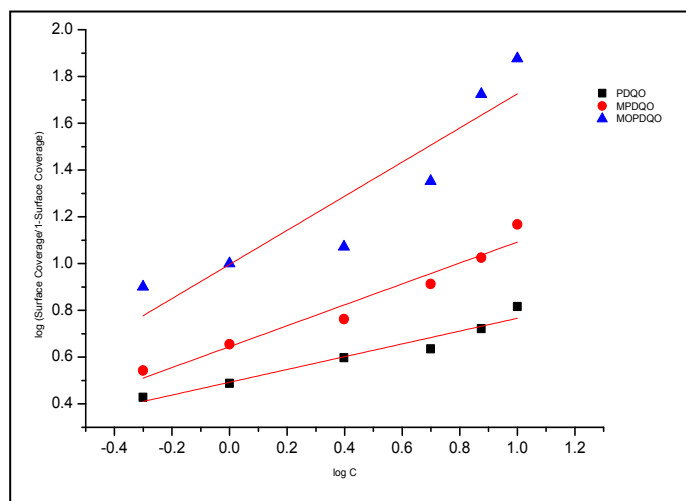**Figure 6 :** Flory-Huggin's plot for the inhibition of corrosion of mild steel in 1M H_2SO_4

Figure 7: El-Awady plot for the inhibition of corrosion of mild steel in 1M H_2SO_4

The plot gives straight lines which show that the experimental data fits the isotherm. The values of K_{ads} and 1/y calculated from the El-Awady isotherm model is listed in Table 4. The values of 1/y are greater than unity confirming that the inhibitor occupies more than one active site.

3.2 Electrochemical Measurements
3.2.1 Potentiodynamic Polarization Studies
The potentiodynamic polarization curves for mild steel in 1M H_2SO_4 in the presence and absence of inhibitor are shown in Figure 8. The investigated inhibitors retard the anodic dissolution of mild steel and cathodic hydrogen discharge reactions. Electrochemical parameters such as current density (I_{corr}), corrosion potential (E_{corr}), Tafel constants (b_a & b_c) and inhibition efficiency were calculated from the Tafel plots and are given in Table 5.

Table 5: Corrosion parameters for corrosion of mild steel with selected concentrations of the inhibitors in 1M H_2SO_4 by Potentiodynamic polarization method

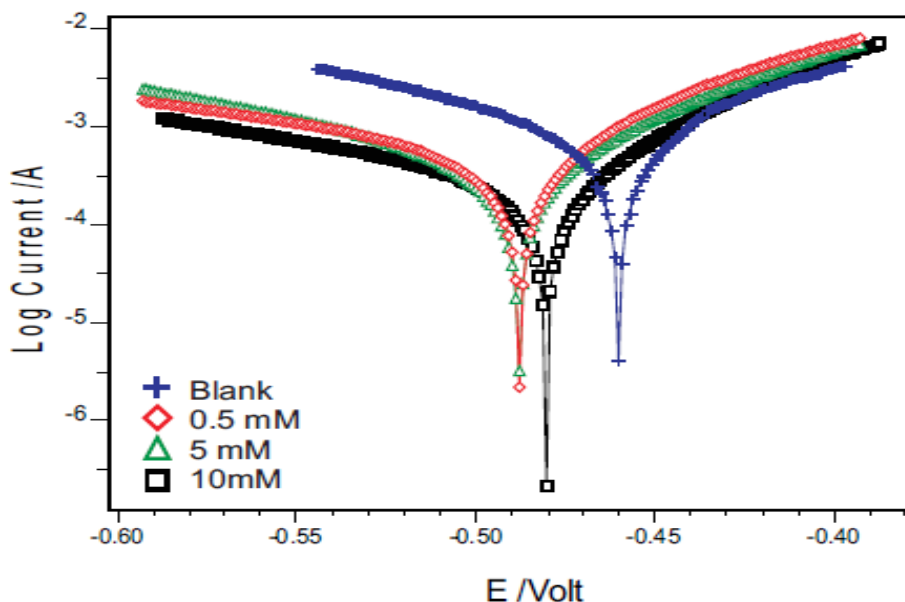| Name of the inhibitor	Con (mM)	Tafel slopes (mV/dec)		$-E_{corr}$ (mV)	I_{corr} ($\mu Amp\ cm^{-2}$)	Inhibition Efficiency (%)
		b_a	b_c			
BLANK	-	69	101	460.1	789.4	-
PDQO	0.5	63	140	490	485.5	38.50
	5.0	61	138	488.4	344.2	56.40
	10.0	57	146	475.8	325.1	58.82
MPDQO	0.5	52	135	469.9	387.0	50.98
	5.0	61	147	490.4	346.5	56.11
	10.0	58	139	484.4	321.7	59.25
MOPDQO	0.5	70	154	489.8	557.6	29.36
	5.0	66	117	486.6	430.2	45.50
	10.0	59	144	480.9	304.5	61.43

Figure 8: Potentiodynamic Polarization curves for mild steel recorded in 1M H_2SO_4 for selected concentrations of the inhibitor (MOPDQO)

From the analysis of the results in Table 5, the following conclusions were made:
(a)   It is observed that the current density for all the inhibitors decreases with increasing in the concentration of inhibitors. This indicates that the inhibitors are adsorbed on the metal surface and hence inhibition occurs. Maximum decrease in I_{corr} values was observed for compound MOPDQO indicating that it is the most effective corrosion inhibitor.
(b)   It is clear that there is no definite trend in the shift of E_{corr} in the presence of corrosion inhibitor. Therefore the synthesized inhibitors can be arranged as a mixed-type inhibitor and the inhibition action is caused by geometric blocking effect [30]. The inhibition action comes from the reduction of the reaction area on the surface of the corroding metal.
(c)   Tafel slopes (b_a and b_c) are significantly affected by the addition of inhibitors. Both b_a and b_c are parallel and are shifted to more negative and positive direction respectively by the addition of inhibitors. This indicates that the mechanism of the corrosion reaction does not change and the corrosion reaction is inhibited by a simple adsorption mode [31]. In other words, the inhibitor has decreased the active surface area for the acid corrosion attack without affecting the mechanism of corrosion and only caused inactivation of a part of the metal surface with respect to the corrosive medium.

3.2.2. Electrochemical impedance spectroscopy

EIS measurements have been carried out at 303 K in acidic solution with and without inhibitors. The charge transfer resistance (R_t) values are calculated from the difference in impedance at lower and higher frequencies. The electrochemical impedance results of different concentrations of the synthesized 1,4-dihydroquinoxaline-2,3-dione derivatives in 1M H_2SO_4 clearly shows semicircle shaped Nyquist plots with increasing radii with increasing concentration of the inhibitors (Figure 9). The appearance of single semi-circle in all the cases corresponds to one capacitive loop [32]. It is apparent form these plots that the impedance response of mild steel in uninhibited H_2SO_4 has significantly changed after the addition of the inhibitors into the corrosive solutions.
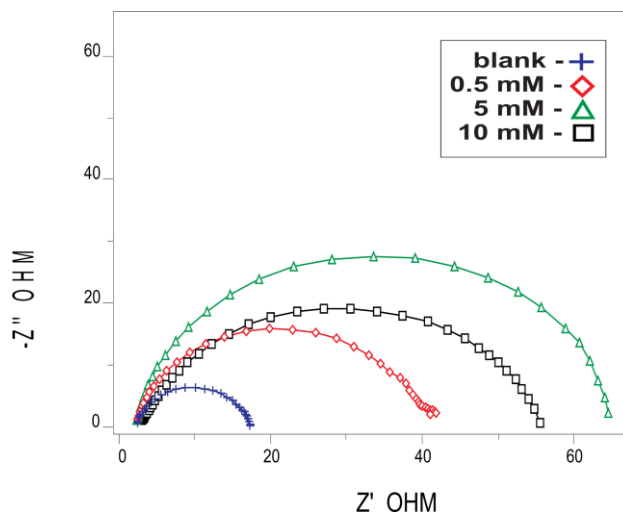

Figure 9: Nyquist diagram for mild steel in 1M H_2SO_4 for selected concentrations of the inhibitor (MOPDQO)

Table 6: AC-impedance parameters for corrosion of mild steel for selected Concentrations of the inhibitors in 1M H_2SO_4

Name of the inhibitor	Con (mM)	R_t (ohm cm^2)	C_{dl} (μF cm^{-2})	Inhibition efficiency (%)
BLANK	-	11.06	27.8	-
PDQO	0.5 5.0 10	32.15 39.38 54.90	34.0 33.4 28.5	65.60 71.91 79.85
MPDQO	0.5 5.0 10	44.22 55.72 62.29	30.6 30.1 24.3	74.99 80.15 82.24
MOPDQO	0.5 5.0 10	35.20 53.64 64.56	31.5 26.7 26.5	68.58 79.38 82.87

As it can be seen from the Table 6, the following results were observed:
(a)   It can be clearly seen that the R_t value increased with increase in the concentration of the inhibitors, leading to an increase in the corrosion inhibition efficiency.
(b)   The values of C_{dl} decreased with an increase in the inhibitors concentration leading to an increase in inhibition efficiency [33]. This situation is the result of an increase in the surface coverage by the inhibitor, which lead to an increase in the inhibition efficiency. The decrease in the C_{dl} Value can result from a decrease in local dielectric constant and/or an increase in the thickness of the electrical double layer, signifying that quinoxaline molecule acts by adsorption at the solution / interface.

The EIS studies clearly indicate that the inhibitor MOPDQD is a good corrosion inhibitor for mild steel in H_2SO_4 medium. The efficiency of the inhibitor increased with increase in inhibitor concentration. Similar to the MOPDQD, the other inhibitors also showing semicircle shaped Nyquist plots and ascertains their capacity to

inhibit the corrosion of mild steel. EIS impedance study also confirms the inhibiting character of inhibitors obtained with polarization curves and weight loss measurements in 1M H_2SO_4.

3.5 Surface Morphology
3.5.1 Scanning electron microscopy (SEM) studies

The mild steel specimens immersed in the blank acid (1M H_2SO_4) and inhibited acid (1M H_2SO_4 + 10 mM of the selected inhibitors MOPDQD) were observed under a scanning electron microscope and the

photographs are shown in Figure 10. Clear examination of SEM images reflects that the surface of the MS in the absence of the inhibitors was found to be corroded more, and the corrosion damages were observed in the form of large pits. The photographs show that the mild steel was heavily corroded in 1M H_2SO_4 where as in the presence of inhibitor the surface condition was comparatively better (Figure 10). This shows that the inhibitor molecules hinder the dissolution of mild steel by forming surface adsorbed layer and thereby reducing the corrosion rate. It also confirms that the inhibitors effectively control the corrosion phenomenon by blocking the active corrosion causing sites on the mild steel surface.
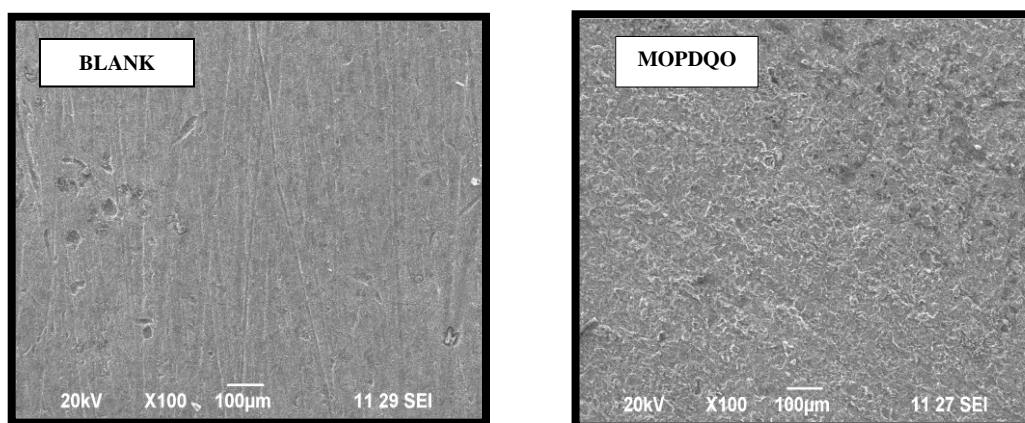
Figure 10: Scanning Electron Microscopy photographs in the presence and absence of the inhibitor

3.5.2 Energy Dispersion Spectroscopy (EDS) studies

The EDX spectra were used to determine the elements present on the surface of mild steel in the uninhibited and inhibited 1M H_2SO_4. The EDX analysis of uninhibited mild steel plate indicate the presence of only Fe and oxygen confirming that passive film on the mild steel surface contained only Fe_2O_3 (Figure 11a). Figure.11b portrays the EDX analysis of mild steel in 1M H_2SO_4 in the presence of inhibitor (MOPDQD). This EDX spectrum shows additional lines due to C (owing to the carbon atoms in the benzene ring), O and N [34]. This spectrum confirms the presence of the inhibitor molecules on mild steel surface. A comparable elemental distribution is shown in Table 7.

Table 7: Surface composition of mild steel after 3h of immersion in 1M H_2SO_4 without and with the optimum concentrations of the studied inhibitors

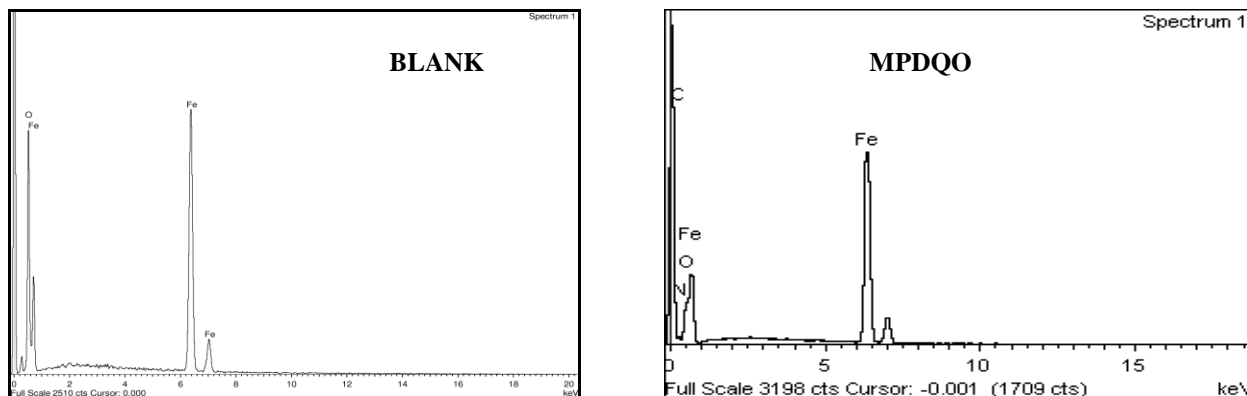| Name of the Inhibitor	Element	Weight (%)	Atomic Weight (%)
BLANK	O	33.80	64.05
	Fe	66.20	35.95
MOPDQO	C	7.07	18.09
	N	6.02	13.21
	O	15.22	29.24
	Fe	71.69	39.46

Figure 11: EDAX analysis of mild steel surface after 3 hour of immersion in 1M H_2SO_4 in the absence and presence of inhibitor (MOPDQO)

3.5.3. FT-IR studies

FT-IR studies were used to confirm the formation of protective layer of inhibitor on the mild steel surface of inhibitors and to provide the possible interactions between the organic molecules and the mild steel surface. The FT-IR spectrum of pure compound MPDQD shows broad band in the region 3400-3300 cm^{-1} which is attributed to –NH stretching vibration. The absorption band at 1669.46 cm^{-1} is characteristic of >C=O stretching vibration In the IR spectrum of the plate immersed in 1M H_2SO_4 and 10mM MPDQD (Figure 12), appearance of a weak band around 3400 – 3300 cm^{-1} and shift of >C=O band from 1669 cm^{-1} to higher wave numbers 1678 cm^{-1} (Figure 12) clearly proved that the electron centres –NH and >C=O are involved in the sharing of electrons with metal.
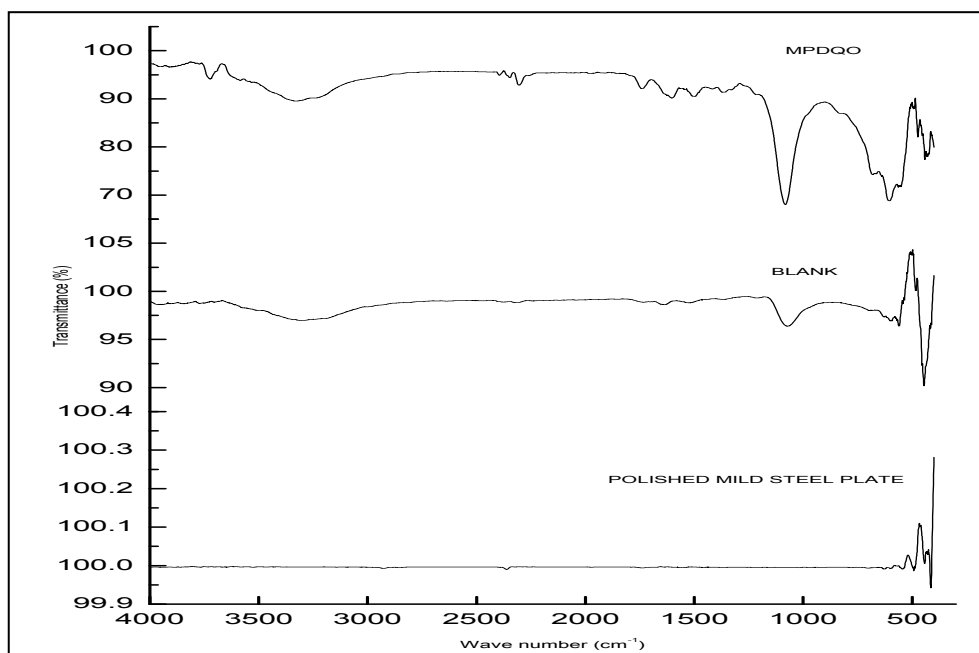

Figure 12: FT-IR Spectra for Polished Mild Steel, Blank and Inhibitor (MPDQO)

These changes support the argument that the imine nitrogen and carbonyl oxygen atoms are coordinated with Fe^{2+}. Furthermore the intensities of these stretching frequencies are decreased confirming the absorption of MPDQO on the metal surface.

3.6. Quantum chemical studies

Density functional theory (DFT) has been used to analyse the characteristics of the inhibitor/surface mechanism and to describe the structural nature of the inhibitor in the corrosion process. It is considered to be a

very useful technique to probe the inhibitor/surface interaction as well as to analyse the experimental data. This technique has been found to be successful in providing insights into the chemical reactivity and selectivity in terms of global parameters such as electronegativity, hardness, softness, fraction of electrons transferred, etc.

The design of the compounds (PDQO, MPDQO and MOPDQD) as a corrosion inhibitor was based on several factors. First, the molecule contains nitrogen and oxygen atoms as active centre. These inhibitors can be easily synthesized and characterized. The optimized molecular structure of the synthesized compound is shown in Figure 13.

The energy difference between the HOMO and LUMO (ΔE) provides information about the overall reactivity of the molecule, the smaller the ΔE value is, the greater is the reactivity of the molecule [35]. The ΔE values of the studied compounds show that MOPDQD (ΔE = 3.76 eV) is more reactive than MPDQD (ΔE = 3.94 eV) and PDQO (ΔE = 4.03 eV) Therefore on interaction with the metal surface, MOPDQD would have the highest tendency to interact with the metal surface. MOPDQD has highest electron density centres due to the presence of –O-CH$_3$ group in comparison to other compounds.

Absolute hardness and softness are important properties to measure the molecular stability and reactivity. A hard molecule has a large energy gap and a soft molecule has a small energy gap. Soft molecules are more reactive than hard ones because they can easily offer electrons to an acceptor. For the simplest transfer of electrons adsorption could occur at the part of the molecule, where the softness value is high [36]. In corrosion process the inhibitor acts as a Lewis base and the metal acts as a Lewis acid. Bulk metals are soft acids and thus soft base inhibitors are most effective for anodic corrosion of these metals [37]. In the present study MOPDQD has higher σ value (0.53) and lower η value (1.88). Normally, the inhibitor with the least value of global hardness η and highest value of global softness σ is expected to have the highest inhibition efficiency [38].
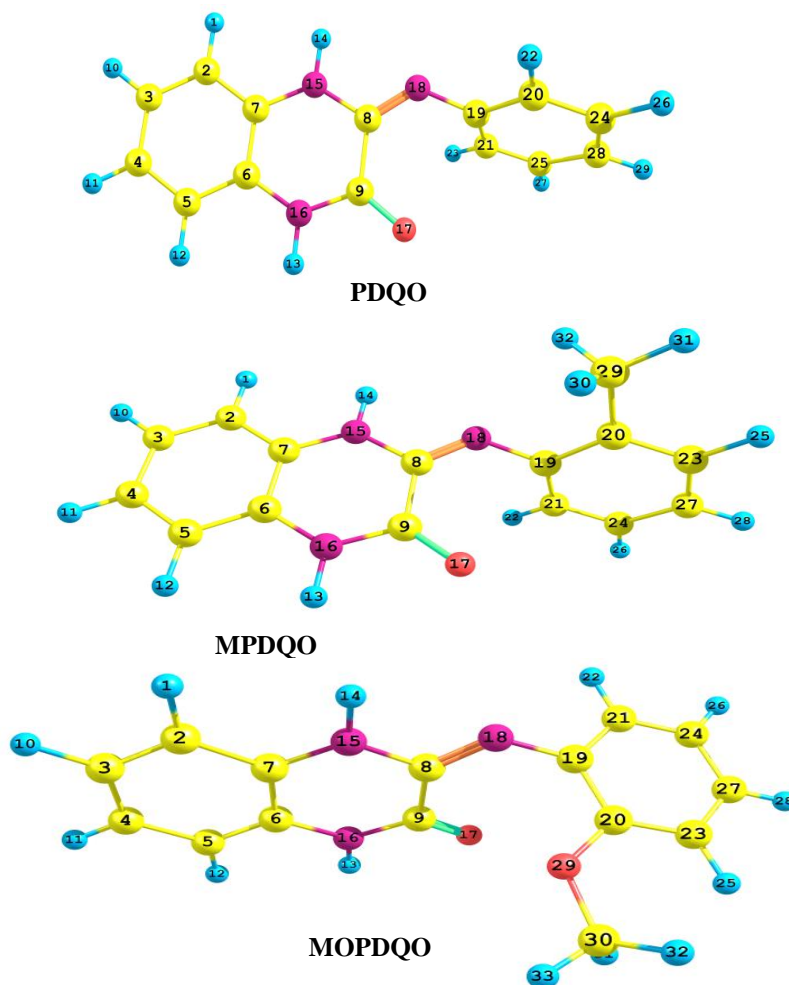

Figure 13: Optimized structure of the studied molecules obtained by B3LYP/6-311G level.

Table 8: The calculated quantum chemical parameters for the selected inhibitors obtained using DFT at the B3LYP/6-311G (d,p) basis set.

Quantum Chemical Parameters	PDQO	MPDQO	MOPDQO
Total energy (amu)	-779.8	-819.13	-894.36
Dipole moment(μ)	4.77	4.89	4.25
E_{HOMO} (eV)	-5.64	-5.55	-5.26
E_{LUMO} (eV)	-1.61	-1.61	-1.5
Energy gap (eV)	4.03	3.94	3.76
Ionization potential (I)	5.64	5.55	5.26
Electron affinity (A)	1.61	1.61	1.5
Hardness (η)	2.02	1.97	1.88
Softness (σ)	0.50	0.51	0.53
Electronegativity (χ)	3.625	3.58	3.38
Fraction of electrons transferred (ΔN)	0.8375	0.8680	0.9628

The number of electrons transferred ΔN indicates the tendency of a molecule to donate electrons. The higher the value of ΔN, the greater is the tendency of a molecule to donate electrons to the electron poor species. In the case of corrosion inhibitors the higher value of ΔN implies a greater tendency to interact with the metal surface. The inhibitor MOPDQD has a higher ΔN value of 0.9628 in comparison to the other inhibitors. Theoretically MOPDQD is expected to exhibit the highest %inhibition efficiency. The values of ΔN follows the order MOPDQD > MPDQD > PDQO. The trend in ΔN values coincides with the experimental results.

Mulliken atomic charges and Fukui functions

The use of Mulliken population analysis to estimate the adsorption centers of inhibitors has been widely reported and it is mostly used for the calculation of charge distribution over the whole skeleton of the molecule [39]. There is a general consensus by several authors that the more negatively charged hetero atom is, the more is its ability to adsorb on the metal surface through a donor-acceptor type reaction [40-42]. It is important to consider the situation corresponding to a molecule that is going to receive a certain amount of charge at some centre and is going to back donate a certain amount of charge through the same centre or another one. Parr and Yang proposed that larger value of Fukui function indicate more reactivity [43].

The Mulliken charge distributions of the studied compounds together with the calculated Fukui indices are presented in Tables 9a-9c. The parameters were calculated for C, N and O atoms. It has been reported that as the Mulliken charges of the adsorbed centre become more negative, more easily the atom donate its electrons to the unoccupied orbital of the metal [44]. From the Tables 9a-9c, it is clear that nitrogen, oxygen and sulphur atoms have high charge densities. The regions of high charge densities are generally the sites to which electrophiles can attach [45]. Therefore N and O atoms are the active centres which have the strongest ability to bond the metal surface.

For a finite system such as an inhibitor molecule, when the molecule is accepting electrons one has f_k^+, the index for nucleophilic attack; when the molecule is donating electrons, one has f_k^-, the index for electrophilic attack. It is possible to observe from Tables 9a-9c that N15; N15 and N15, O29 are the most preferred sites for nucleophilicity for PDQO, MPDQO and MOPDQO respectively. They have highest f_k^+ value.

On the other hand N16, O17, N18; N16, O17, N18 and N16, O17, N18 are the most preferred sites for electrophilicity for PDQO, MPDQO and MOPDQO respectively. They have highest f_k^- value. These results confirm the possibility of donation and back-donation of electrons between the inhibitors and the mild steel [46].

Saranya et al.

Table 9a: Calculated Mulliken atomic charges, Fukui functions and softness indices for the atoms of PDQO using DFT at the B3LYP/6-311G(d,p) basis set
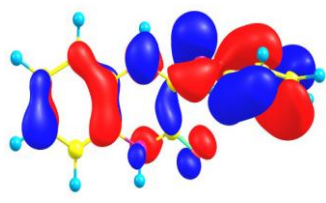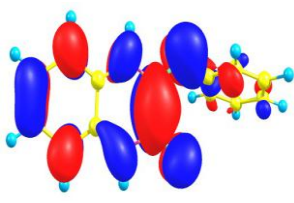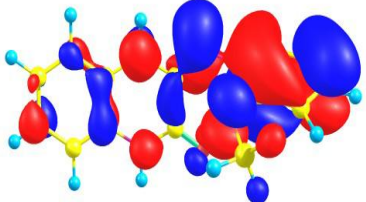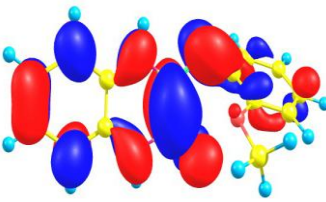
Atoms	q_N	q_{N+1}	q_{N-1}	f_k^+	f_k^-	f_k^0	s_k^+	s_k^-
C2	0.0177	0.0808	-0.0854	0.0631	0.1031	0.0831	0.0316	0.0515
C3	0.0051	0.0676	-0.0716	0.0625	0.0767	0.0696	0.0312	0.0384
C4	-0.0014	0.0786	-0.0778	0.0800	0.0764	0.0782	0.0400	0.0382
C5	0.0276	0.0839	-0.0773	0.0563	0.1049	0.0806	0.0281	0.0524
C6	0.1870	0.2106	0.1904	0.0237	-0.0034	0.0101	0.0118	-0.0017
C7	0.1966	0.1978	0.1957	0.0011	0.0009	0.0010	0.0006	0.0005
C8	0.2689	0.3134	0.1962	0.0445	0.0727	0.0586	0.0223	0.0364
C9	0.3522	0.3808	0.2562	0.0286	0.0961	0.0623	0.0143	0.0480
N15	-0.2343	-0.1655	-0.2763	0.0687	0.0420	0.0554	0.0344	0.0210
N16	-0.2323	-0.1881	-0.2778	0.0442	0.0454	0.0448	0.0221	0.0227
O17	-0.3143	-0.2864	-0.4129	0.0278	0.0987	0.0632	0.0139	0.0493
N18	-0.3628	-0.3124	-0.4539	0.0504	0.0911	0.0708	0.0252	0.0456
C19	0.0574	0.0555	0.0999	-0.0018	-0.0425	-0.0222	-0.0009	-0.0213
C20	0.0194	0.1194	-0.0324	0.1000	0.0518	0.0759	0.0500	0.0259
C21	0.0445	0.1335	0.0217	0.0890	0.0228	0.0559	0.0445	0.0114
C24	-0.0089	0.0604	-0.0552	0.0693	0.0463	0.0578	0.0346	0.0232
C25	-0.0113	0.0568	-0.0592	0.0681	0.0479	0.0580	0.0340	0.0239
C28	-0.0112	0.1133	-0.0803	0.1245	0.0691	0.0968	0.0622	0.0346

Table 9b: Calculated Mulliken atomic charges, Fukui functions and softness indices for the atoms of MPDQO using DFT at the B3LYP/6-311G(d,p) basis set
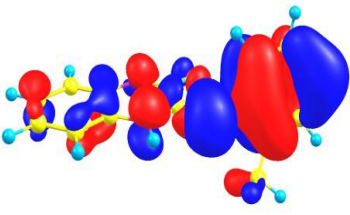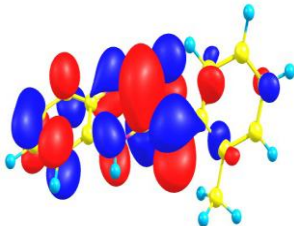
Atoms	q_N	q_{N+1}	q_{N-1}	f_k^+	f_k^-	f_k^0	s_k^+	s_k^-
C2	0.0170	0.0763	-0.0844	0.0593	0.1014	0.0803	0.0302	0.0517
C3	0.0052	0.0636	-0.0705	0.0584	0.0758	0.0671	0.0298	0.0386
C4	-0.0014	0.0736	-0.0774	0.0750	0.0760	0.0755	0.0382	0.0388
C5	0.0275	0.0806	-0.0762	0.0531	0.1038	0.0784	0.0271	0.0529
C6	0.1863	0.2076	0.1897	0.0213	-0.0035	0.0089	0.0109	-0.0018
C7	0.1968	0.1958	0.1957	-0.0010	0.0011	0.0001	-0.0005	0.0005
C8	0.2700	0.3121	0.1995	0.0422	0.0705	0.0563	0.0215	0.0360
C9	0.3520	0.3769	0.2573	0.0248	0.0948	0.0598	0.0127	0.0483
N15	-0.2367	-0.1715	-0.2778	0.0652	0.0410	0.0531	0.0333	0.0209
N16	-0.2323	-0.1894	-0.2771	0.0430	0.0447	0.0439	0.0219	0.0228
O17	-0.3149	-0.2916	-0.4132	0.0233	0.0984	0.0608	0.0119	0.0502
N18	-0.3742	-0.3318	-0.4627	0.0424	0.0885	0.0655	0.0216	0.0451
C19	0.0626	0.0776	0.0999	0.0150	-0.0372	-0.0111	0.0076	-0.0190
C20	-0.0726	-0.0494	-0.0866	0.0233	0.0140	0.0186	0.0119	0.0071
C21	0.0523	0.1370	0.0313	0.0847	0.0210	0.0529	0.0432	0.0107
C23	-0.0055	0.0673	-0.0533	0.0728	0.0479	0.0603	0.0371	0.0244
C24	-0.0128	0.0619	-0.0586	0.0747	0.0459	0.0603	0.0381	0.0234
C27	-0.0084	0.1154	-0.0759	0.1238	0.0676	0.0957	0.0631	0.0345
C29	0.0891	0.1879	0.0405	0.0988	0.0485	0.0737	0.0504	0.0248

Table 9c: Calculated Mulliken atomic charges, Fukui functions and softness indices for the atoms of MOPDQO using DFT at the B3LYP/6-311G(d,p) basis set

Atoms	q_N	q_{N+1}	q_{N-1}	f_k^+	f_k^-	f_k^0	s_k^+	s_k^-
C2	0.0164	0.0732	-0.0829	0.0567	0.0993	0.0780	0.0301	0.0526
C3	0.0029	0.0581	-0.0698	0.0552	0.0727	0.0639	0.0292	0.0385
C4	-0.0037	0.0670	-0.0798	0.0707	0.0761	0.0734	0.0375	0.0403
C5	0.0243	0.0742	-0.0763	0.0499	0.1005	0.0752	0.0264	0.0533
C6	0.1870	0.2048	0.1899	0.0178	-0.0029	0.0075	0.0094	-0.0015
C7	0.1960	0.1922	0.1954	-0.0038	0.0007	-0.0016	-0.0020	0.0003
C8	0.2928	0.3333	0.2203	0.0405	0.0725	0.0565	0.0215	0.0384
C9	0.3686	0.3885	0.2811	0.0199	0.0876	0.0537	0.0105	0.0464
N15	-0.2389	-0.1756	-0.2784	0.0633	0.0394	0.0514	0.0335	0.0209
N16	-0.2376	-0.1967	-0.2815	0.0409	0.0439	0.0424	0.0217	0.0232
O17	-0.3280	-0.3104	-0.4211	0.0176	0.0931	0.0553	0.0093	0.0493
N18	-0.3648	-0.3229	-0.4472	0.0420	0.0824	0.0622	0.0222	0.0437
C19	0.0490	0.0632	0.0887	0.0142	-0.0397	-0.0127	0.0075	-0.0210
C20	0.2369	0.2800	0.2139	0.0431	0.0230	0.0330	0.0229	0.0122
C21	0.0155	0.1012	-0.0462	0.0857	0.0617	0.0737	0.0454	0.0327
C23	-0.0278	0.0391	-0.0738	0.0669	0.0460	0.0565	0.0355	0.0244
C24	-0.0140	0.0764	-0.0602	0.0904	0.0462	0.0683	0.0479	0.0245
C27	-0.0139	0.1007	-0.0897	0.1146	0.0758	0.0952	0.0607	0.0402
O29	-0.3724	-0.3340	-0.3481	0.0384	-0.0243	0.0070	0.0203	-0.0129
C30	0.2118	0.2878	0.1657	0.0761	0.0461	0.0611	0.0403	0.0244

Name of the Inhibitor	HOMO	LUMO
PDQO		
MPDQO		
MOPDQO		

3.7. Mechanism of inhibition

The studied compounds show good inhibition efficiencies towards corrosion of mild steel in 1M H_2SO_4. As far as the inhibition process is concerned, it is generally assumed that adsorption of an organic inhibitor at the metal/solution interface is the first step in the action mechanism of the organic compounds in aggressive acidic media. Four types of adsorption may take place during inhibition involving organic molecules at the metal/solution interface:

(i) Electrostatic attraction between charged molecules and the charged metal,

(ii) Interaction of unshared electron pairs in the molecule with the metal,

(iii) Interaction of π-electrons with the metal,

(iv) A combination of the above situations [47,48].

Concerning inhibitors, the inhibition efficiency depends on several factors, such as the number of adsorption sites and their charge density, molecular size, heat of hydrogenation, mode of interaction with the metal surface, and the formation metallic complexes [49].

On the otand, in 1M H_2SO_4, mild steel is corroded in Fe^{2+}, and the surface of MS is positively charged. SO_4^{2-} ions are attracted by the charges on the metal surface which tends to be charged negatively. The obtained results could be explained on the assumption that the negatively charged SO_4^{2-} would attach to the positively charged surface. There may be a synergism between SO_4^{2-} and the protonated inhibitors near the interface, and the concentrations of SO_4^{2-} and that of the neutral forms and the protonated forms of the inhibitors were probably much higher than those in the bulk solution; the protonated forms did attach electrostatically to the negative charges at the metal surface [50-52]. When the neutral forms and the protonated forms of the inhibitors adsorb on the metal surface, coordinate bonds are formed by partial transference of electrons from the unprotonated N atoms, O atoms, delocalized π electrons in the quinoxaline rings to the metal surface via vacant d orbitals of Fe^{2+} ions. So, in the process of adsorption, both physical and chemical adsorptions might take place. The inhibitory mechanism on metal dissolution is related to the chelating effect of Fe^{2+} ions close to mild steel surface. Indeed, it is proven that Fe is corroded to Fe^{2+} in H_2SO_4 solution and no oxide film is formed to protect the surface from corrosion [53,54]. It is also known that the organic compounds can be adsorbed by the interactions between the lone pairs of electrons of nitrogen, or oxygen atoms with metal surface. These processes are facilitated by the presence of d vacant orbitals of low energy in the copper ions, as observed in transition group metals. Recently, it was found that the formation of donor-acceptor surface complexes between free electrons of an inhibitor and a vacant d orbital of a metal is responsible for the inhibition corrosion process [55]. The number of Fe^{2+} ions in proximity of copper increases with increasing temperature, leading to the formation of Fe^{2+} inhibitor complexes protective film (increase in surface coverage) which creates a physical barrier between mild steel surface and the electrolyte, retarding the dissolution of the metal [56].

3.8 Evaluation of inhibitors

Inhibition efficiency values obtained for the inhibitors are shown in the following sequence:

MOPDQO > MPDQO > PDQO

The inhibitors MOPDQO, MPDQO showed better inhibition efficiency due to the high electron density group (CH_3, OCH_3) on the phenyl ring. The high inhibition efficiency may be attributed to the preferred flat orientation of these compounds on the metal surface. The interaction occurs between the delocalized π electrons of the two rings, the double bond (-C=N-) and the lone pair of electrons on N and O atoms with the positively charged metal surface [57]. Among the three inhibitors MOPDQO exhibit high inhibition efficiency. The best performance of MOPDQO may be due to the presence of $-O-CH_3$ group which increase further its electron densities for their adsorption on the metal surface. MPDQO is also expected to exhibit high inhibition efficiency due to the presence of $-CH_3$ group.

Conclusion

1. The investigated 1,4-dihydroquinoxalin-2,3-dione derivatives are fond to perform well as corrosion inhibitors in 1M H_2SO_4 solution. The order of inhibition as follows

   MPODQO > MPDQO > PDQO

2. The inhibition efficiency increases with increase in the concentration but decreases with rise in temperature.

3. The adsorption of quinoxalines on mild steel from 1M H_2SO_4 obeys Langmuir adsorption isotherm.

4. Phenomenon of physical adsorption is proposed from the value of kinetic/ thermodynamics parameters (E_a, ΔG_{ads}) obtained.
5. The polarization data indicates that the inhibitors behave as mixed – type.
6. Quantum mechanical studies of the Quinoxaline derivatives were found to be in good agreement with the experimental results

References

1. Lebrini M., Lagrenée M., Traisnel M., Gengembre L., Vezin H., Bentiss F., *App. Surf. Sci*. 253 (23) (2007) 9267–9276.
2. Sudhish Kumar Shukla , Quraishi M A., *Corros. Sci.* 51 (9) (2009) 1990–1997.
3. Ying Yan., Weihua Li., LankunCai., BaorongHo., *Electrochimica Acta*. 53 (20) (2008) 5953–5960.
4. Okafor P C., Liu C B., Zhu Y J., Zheng Y. G., *Ind. Eng. Chem. Res*. 50 (12) (2011) 7273–7281
5. Khaled K F., Al-Qahtani M M., *Mater.Chem.Phys*. 113(1) (2009)150-158
6. Khadija Hnini, Salah Fadel, Molay Abderrahim El Mhammedi, Abdelilah Chtaini, El Mostapha Rakib., *Leonardo Electronic Journal of Practices and Technologies.* 12 (2008)1-14.
7. Chakravarthy M P., Mohana K N., *Int.J of Corros*. Article ID 854781 (2013) 13 pages http://dx.doi.org/10.1155/2013/854781
8. Kosari A., Momeni M., Parvizi R., Zakeri M., Moayed M H., Davoodi A., Eshghi H., *Corros. Sci* 53 (2011) 3058–3067.
9. Obot I B., Obi-Egbedi N O., Odozi N W., *Corros. Sci.* 52 (2010) 93.
10. Obot I B., Obi-Egbedi N O., *Mater. Chem. Phys*. 122 (2010) 325.
11. Obot I B., Obi-Egbedi N O., *Corros. Sci.* 52 (2010) 282.
12. Hammouti B., Zarrouk A., Al-Deyab S S., Warad I., *Oriental. J.Chem.* 27 (2011) 23.
13. Elayyachy M., Hammouti B., A.El Idrissi, Aouniti A., *Port. Electrochim. Acta.* 29 (2011) 57.
14. El Ouali I., Hammouti B., Aouniti A., Benabdellah M., Kertit S., *Der Pharma. Chem*. 3 (2011) 294.
15. Benabdellah M., Touzani R., Aouniti A., Dafali A., Elkadiri S., Hammouti B., Benkaddour M., *Phys.Chem.News.* 43 (2008) 115.
16. Zarrouk A., Dafali A., Hammouti B., Zarrouk H., Boukharis S., Zertoubi M., *Int. J. Electrochem. Sci.* 5 (2010) 46.
17. El-Ouali I., Hammouti B., Aouniti A., Ramali Y., Azougagh M., Essassi E.M., Bouachrine M., *J. Mater. Environ. Sci.* 1 (2010) 1.
18. Lopez N., Illas F., *J.Phys. Chem*., B102 (1998) 1430.
19. Durnie W., De Marco R., Kinsella B., Jsfferson A., Pejcic B., *J.of.Electrochem.Soc*., 152 (2005) B1
20. Ahmed Y. Musa., Ramzi T.T. Jalgham , Abu Bakar Mohamad., *Corros. Sci,* 56 (2012) 176–183.
21. Lutendo C. Murulana , Ashish K. Singh , Sudhish K. Shukla , Mwadham M. Kabanda , Eno E. Ebenso., *Ind. Eng. Chem. Res*., 51 (40) (2012) 13282–13299.
22. Gomma M K., Wahdan M H*., Mater. Chem. Phys*. 39 (1995) 209.
23. Marsh J., *Advanced Organic Chemistry, 3rd Ed.,* Wiley Eastern, New Delhi, (1988).
24. Khamis E., Hosney A., El-Khodary S., Afinidad., *Rev. Quim. Teor. Aplic*. 456 (1996) 95.
25. El-Etre A Y., Corros. Sci., 45 (2003) 2485-2495.
26. Beulah Thavamani Esther Rani J R., Jeyaraj T., *Der Chemica Sinica.* 3(6) (2012) 1358-1368
27. Singh A K., Shukla S K., Singh M., Quraishi M A., *Mater. Chem. Phys*., 129 (2011) 68-76.
28. Ibot I B., Obi-Egbedi N O., Umoren S A., Int. J. Electrochem. Sci. 4 (2009) 863.
29. Singh A K., Quraishi M A., Corros.Sci, 53 (2011) 1288.
30. Cao C., *Corros. Sci,* 38 (1996) 2073.
31. Khaled K F., Saedah R.Al-Mhyawi*., Int. J. Electrochem. Sci.* 8 (2013) 4055-4072.
32. Yurt A., Balaban A., Kandemir S., Bereket G., Erk B., *Mater. Chem. Phys*. 85 (2004) 420- 426.
33. Fenging Xu, Baorong Hou., *Acta Metallugica Sinica.* 22 (4) (2009) 247-254.
34. Maqsood Ahmad Malik, Mohd Ali Hashim, Firdosa Nabi, Shaeel Ahmed Al-Thabaiti, Zaheer Khan., *Int.J.Electrochem.Sci.* 6 (2011) 1927-1948.
35. Bentiss F, Traisnel M, Vezin H, Hildebran H F., Lagrenee M., *Corros. Sci*. 46 (2004) 2781
36. Eddy M O, *Mol. Simul.,* 35 (5) (2010) 354
37. Hasanov R, Sadiklgu M, Bilgic S., *Appl. Surf. Sci.* 253 (2007) 3913
38. Ebenso E E., Isabirye D A., Eddy N O., *Int. J. Mol. Sci.,* 11 (2010) 2473.
39. Bentiss F., Lebrini M., Lagrenee M., Traisnel M., Elfarouk A., Vezin H., *Electrochim. Acta* 52 (2007) 6865.

40. Obot I B., Obi-Egbedi N O., Odozi N W., *Corros. Sci.* 52 (2010) 923
41. Obot I B., Obi-Egbedi N O., *Corros. Sci.* 52 (2010) 282
42. Fang J., Li J*., J.Mol.Struct.* (THEOCHEM) 593 (2002) 179.
43. Obot I B., Obi-Egbedi N O., *Colloids and Surfaces A: Physicochem. Eng. Aspects.* 330 (2008) 207.
44. Xia S, Qiu M, Yu L, Liu F, Zhao.H., *Corros.Sci*., 50 (2008) 2021-2029.
45. Musa A Y., Kadhum A H., Mohamad A B., Rahoma.A B., Mesmari H., *J. Mol. Struct*., 969 (2010) 233-327.
46. Obi-Egbedi N O., Obot I B., El-Khaiary M I., Umoren S A., Ebenso E E., *Int. J. Electrochem. Sci.* 6 (2011) 5649-5675.
47. Schweinsberg D P., George G A., Nanayakkara A K., Steinert D A., *Corros.Sci*, 28 (1) (1998) 33–42.
48. Fouda A S., Moussa M N., Taha F I., Elneanaa A I., *Corros Sci*, 26 (9) (1986) 719–726.
49. Cicileo G P., Rosales B M., Varela F E., Vilche J R., *Corros Sci*, 41(7) (1999) 1359– 1375.
50. Pourbaix M., *Atlas of Electrochemical Equilibria in Aqueous Solutions*, NACE, 1975.
51. Johnson H E., Leja J., *J.of the Electrochem.Soc*. 112 (6) (1965) 638- 641.
52. Zhang D. Q., Cai Q. R., He X. M., Gao L. X., Kim G. S.*, Mater. Chem. Phys,* 114(2-3) (2009) 612–617.
53. Fouda A. S., El-Awady Y. A., Abo-El-Enien O. M., Agizah F. A., *Anti.Corros Method Mater*. 55(6) (2008) 317-323
54. Ateya B G., Anadouli B E., El-Nizamy F M., *Corros.Sci* (1984) 24509- 24515
55. Niamien P M., Kouassi H A., Trokourey A., Essy F K., Sissouma D.,   Bokra Y., *ISRN Materials Science* (2012) ID 623754   doi:10.5402/2012/623754.
56. Nahle A., Ideisan I. Abu-Abdoun, Abdel-Rahim I, *Int. J. Corros* (2012) 1-7. DOI: 10.1155/2012/380329

(2015); http://www.jmaterenvironsci.com